JOURNAL OF Materials CHEMISTRY

Ferroelectric and antiferroelectric "banana phases" of new fluorinated five-ring bent-core mesogens

Hajnalka Nádasi,[a] Wolfgang Weissflog,[a] Alexey Eremin,[a] Gerhard Pelzl,*[a] Siegmar Diele,[a] B. Das[b] and Siegbert Grande[b]

[a]*Institut für Physikalische Chemie, Martin-Luther-Universität Halle-Wittenberg, Mühlpforte 1, D-06108 Halle/S., Germany*
[b]*Universität Leipzig, Fakultät für Physik und Geowissenschaften, Linnéstraße 5, D-04103 Leipzig, Germany*

Received 17th December 2001, Accepted 13th February 2002
First published as an Advance Article on the web 21st March 2002

Two homologous achiral five-ring mesogens with lateral fluorine substituents on the core and on the outer rings are presented. Both compounds exhibit two B_5 phases and the B_2 phase. The high-temperature B_5 phases possess an antiferroelectric ground state. The low-temperature B_5 phase was found to be ferroelectric, which is indicated by the bistable switching. The assignment and characterization of the mesophases is based on XRD measurements, ^{1}H-, ^{19}F-, ^{13}C-NMR and electro-optical measurements.

Ferroelectricity in liquid crystals has been known since the pioneering work by R. B Meyer *et al.*[1] Chirality in a tilted SmC phase introduced by chiral dopants or by chirality of the constituting molecules themselves results in a breaking of mirror symmetry. In such chiral tilted phases the symmetry group is reduced to C_2. Hence, it permits the appearance of the spontaneous electric polarization $\boldsymbol{P}_s$ in each layer of the SmC* phase. However, in bulk, the equilibrium structure will be twisted into a helix so that the polarization of the layers precesses around the layer normal and in a macroscopic sample the spontaneous polarization averages to zero and a surface-stabilization is required to obtain bistable ferroelectric (FE) switching. Later antiferroelectric (AFE) and ferrielectric (FI) smectic phases were also discovered in such materials.[2,3]

Independently from this, several theoretical concepts were developed in order to obtain ferroelectric smectic phases built up by achiral molecules. Prost and Barois[4] and Petschek and Wiefling[5] predicted a ferroelectric SmA phase where the spontaneous polarization is directed along the normal of the smectic layers. In tilted smectic phases formed by achiral molecules the vector of the spontaneous polarization must be in the tilt plane[5,6] or in the layer plane.[7] Lin[8] suggested the formation of polar columnar phases from bow-like molecules with dipole moments directed along the column axis. The first experimental evidence of ferroelectricity in a non-chiral tilted smectic phase was reported by Tournilhac *et al.*[9] in polyphilic compounds. The mechanism by which the polar phase is generated differs from that found in conventional chiral smectics. In the case of polyphilic compounds chemically different moieties of a molecule tend to segregate to form polar smectic layers and should in principle allow the preparation of a phase in which the bulk polarization is parallel to the long axis of the constituent molecules. Later Soto Bustamente *et al.*[10] described antiferroelectric behavior in a mixture of an achiral side-chain polymer with its monomer. In both cases a spontaneous polarization could be detected by pyroelectric measurements but no electro-optical switching was observed.

A very successful concept for ferro- or antiferroelectric smectic phases is based on achiral bent-shaped molecules.[11] Because of the close packing of bent molecules and high rotational hindrance about the long molecular axis an in-layer polar order emerges despite the achiral nature of the molecules. It was found that in the most frequently investigated phase—the so-called B_2 phase—the ground state is an antiferroelectric one, which means that the polar direction which coincides with the bent direction alternates from layer to layer. This antiferroelectric ground state can be switched into ferroelectric states.[12–15] Detailed electro-optical investigations by Link *et al.*[15] gave evidence that the polar packed molecules are tilted with respect to the layer normal. This combination of tilt and polar order in the smectic layers leads to a chirality of the smectic layers as a whole. Two distinct domains could be distinguished. In the first type the sign of the chirality alternates from layer to layer, therefore these domains were designated as racemic ones. In the second type the chirality remains uniform so that macroscopic chiral domains result. These domains were designated as homogeneously chiral.[15] It should also be noted that other switchable "banana phases" could be detected which are designated by the code letters B_5 and B_7 and which also exhibit an antiferroelectric ground state.[13,16] Walba *et al.*[17] at first reported a B_7 phase with a ferroelectric ground state which shows bistable switching like a chiral SmC* phase.

Recently Nguyen *et al.*[18] presented new achiral five-ring banana-shaped compounds with fluorine substituents of the terminal rings which exhibit four switchable smectic phases. The existence ranges of these phases but also the transition enthalpies between them are rather low. All these phases have liquid-like order within the smectic layers, but structural differences are not reported.

In this paper we present two homologous five-ring bent-core mesogens with lateral fluorine substituents on the central core as well as on the outer rings. These compounds not only exhibit a B_2 phase but also several switchable higher ordered "banana phases". The structural characterization was performed by X-ray diffraction measurements completed by NMR and electro-optical investigations. Since the compounds possess fluorine substituents on the central core and the outer rings the orientational order parameter and the conformation of the molecules in the liquid crystalline state could be studied in one experiment using ^{19}F-NMR. Besides antiferroelectric B_5-like phases we were able to detect a low-temperature B_5 phase which possesses a ferroelectric ground state and shows bistable switching.

Materials

The homologous bent-core compounds were prepared as shown in Scheme 1.

 DOI: 10.1039/b111421b

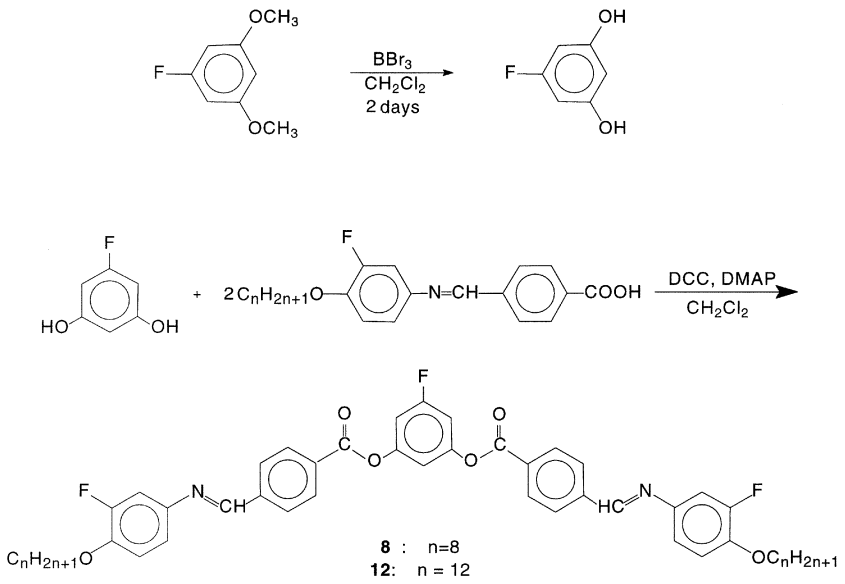

Scheme 1

In the transition schemes the result of phase assignment is anticipated. It should be noted that these materials have already been reported in a review article (ref. 19) but no details concerning the mesophase behaviour are given there.

8: CrI $\underset{[22.9]}{79^{\circ}C}$ CrII $\underset{[2.7]}{113^{\circ}C}$ B_{5F} $\underset{[1.3]}{131^{\circ}C}$ $B_{5A'''}$ $\underset{[1.6]}{135.5^{\circ}C}$ $B_{5A'''}$ $\underset{[0.2]}{137^{\circ}C}$ $B_{5A''}$ $\underset{[0.2]}{138.9^{\circ}C}$ $B_{5A'}$ $\underset{[0.5]}{139.8^{\circ}C}$ B_2 $\underset{[23]}{163.5^{\circ}C}$ I

12: CrI $\underset{[24.6]}{78^{\circ}C}$ CrII $\underset{[18.1]}{87^{\circ}C}$ CrIII $\underset{[1.0]}{112^{\circ}C}$ B_{5F} $\underset{[2.5]}{122.5^{\circ}C}$ B_{5A} $\underset{[0.9]}{128^{\circ}C}$ B_2 $\underset{[24.6]}{157^{\circ}C}$ I

The numbers in square brackets under the transition temperatures designate the transition enthalpies in kJ mol^{-1}. The symbol B_5 is used here as a common designation for all phases which exhibit the structural properties of the B_5 phase described earlier.[13]

Synthetic procedure

Synthesis of 3,5-dihydroxyfluorobenzene. 3,5-Dimethoxyfluorobenzene (1.5 g, 9.6 mmol) was dissolved in dry dichloromethane and purged by nitrogen. Boron tribromide (29 ml, 1 M solution in dichloromethane, 29 mmol) was added to the solution under nitrogen atmosphere at room temperature. Complete conversion to 3,5-dihydroxyfluorobenzene occurred in 2 days.

The reaction was quenched with water and stirred for an additional 30 minutes. The reaction mixture was extracted with ether twice. The combined organic layer was washed with brine and water, dried over Na_2SO_4 and concentrated.

The crude product was recrystallized from toluene to provide a brown crystalline solid (1.08 g, 87.5%): mp 145 °C; R_f 0.13 (1 : 2.5 EtOAc : heptane); ^{1}H-NMR (400 MHz, DMSO) δ = 5.97 (dd, 4 J = 2.2 Hz, 3 $J_{H\text{-}F}$ = 8.8 Hz, 2 H, ArH), 6.04 (m, 4 J = 2.2 Hz, 5 $J_{H\text{-}F}$ = 0.8 Hz, 1 H, ArH), 9.61 (s, 1 H, OH).

Synthesis of 5-fluoro-1,3-phenylene bis[4-(3-fluoro-4-*n*-alkoxyphenyliminomethyl)]benzoate. 3,5-Dihydroxyfluorobenzene (0.14 g, 1.1 mmol), 4-(3-fluoro-4-*n*-alkyloxyphenyliminomethyl)-benzoic acid[19] (2.2 mmol) and DCC (0.54 g, 2.6 mmol) were dissolved in dry dichloromethane. A catalytic amount of DMAP was added to the solution. The reaction mixture was stirred for a week.

The dichloromethane was evaporated, and the crude product was recrystallized twice from DMF with ethanol to provide a yellow powder. Yield (**8**: 55%, **12**: 50%). ^{1}H-NMR (**8**) (400 MHz, $CDCl_3$) δ = 0.86–0.89 (m, 6 H, CH_3), 1.24–1.49 (m, 20 H, $(CH_2)_5CH_3$), 1.79–1.84 (m, 4 H, OCH_2CH_2), 4.05 (t, 3 J = 6.7 Hz, 4 H, OCH_2), 6.96–7.00 (m, 4 H, ArH), 7.04–7.07 (m, 4 J = 2.4 Hz, 5 H, ArH), 7.11 (dd, 4 J = 2.4 Hz, 3 $J_{H\text{-}F}$ = 12.0 Hz, 2 H, ArH), 8.01 (d, 3 J = 8.4 Hz, 4 H, ArH), 8.25 (d, 3 J = 8.4 Hz, 4 H, ArH), 8.53 (s, 2 H, CH=N). MS *m/z*: 834 (M^+, 22), 722 (4), 611 (1), 481 (1), 368 (2), 354 (100), 259 (2), 242 (46), 213 (34), 185 (0,7), 138 (2), 105 (1), 69 (11).

Results

Calorimetric and microscopical investigations

As shown in the DSC curve of compound **12** and **8** all phase transitions (also for mesophases with a small range of existence) could be conclusively detected by calorimetry (Fig. 1). It is noteworthy from the transition scheme that the transition enthalpies between these phases are rather low (0.2–2.5 kJ mol^{-1}) in comparison with the clearing enthalpy.

On cooling the isotropic liquid the mesophase appears as a non-specific grainy texture under the microscope characteristic for the B_2 phase. A kind of schlieren texture could be obtained by shearing the sample. At the transitions into the low-temperature phases the texture does not markedly change. Nevertheless, for a fast heating or cooling rate these phase transitions could be also recognised by a minor change of the textures.

As is discussed later, fan-shaped domains have been obtained using a sufficiently high electric field. At the transition $B_2 \rightarrow B_5$ the fan-shaped texture became more flat. A considerable change was observed at the transition into B_{5F} when a constriction of the texture has been seen and the tapes became broken, but there was no change in texture at the transition into the solid state.

NMR investigations

^{19}F-NMR spectra of the compounds in the liquid crystalline phase consist of a triplet representing the dipole interaction of the fluorine atom on the central ring with the neighbouring two protons and a well separated doublet caused by dipole splitting of the fluorine on the ring *A*. The order parameter *S* can be obtained from the triplet separation. Neglecting the transversal order parameter *D*,[20] the splitting can be written as

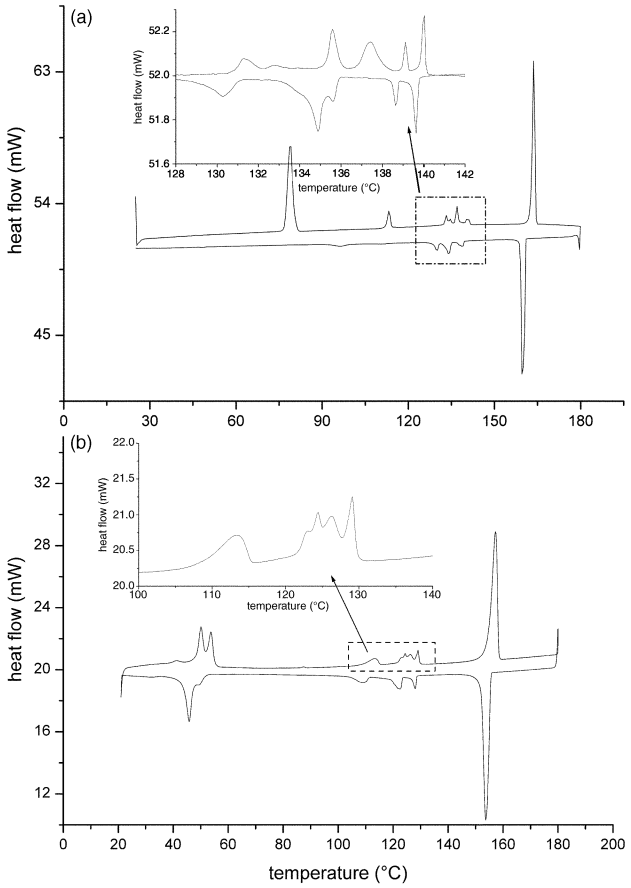

Fig. 1 DSC thermogram of compounds (a) **8** and (b) **12** (heating and cooling run, rate 5.0 K min^{-1}; enlarged region made at the rate 1.0 K min^{-1}).

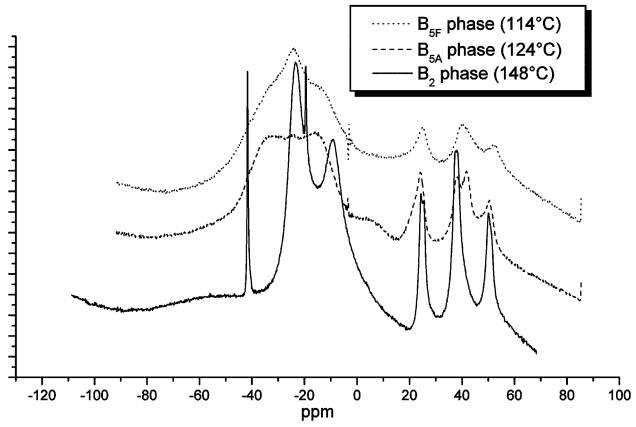

Fig. 2 ^{19}F-NMR spectra of the B_2, B_{5A} and B_{5F} phases of compound **12**.

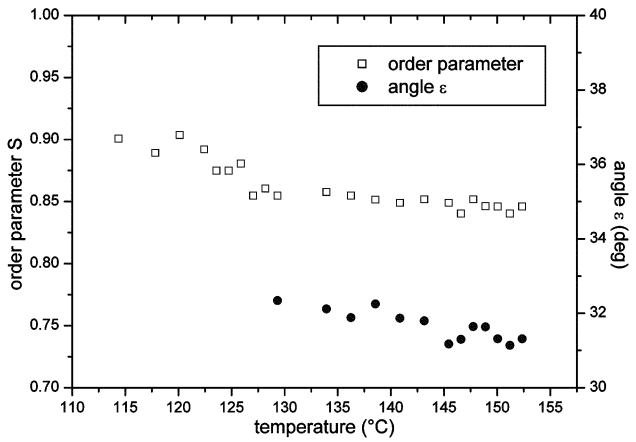

Fig. 3 Temperature dependence of the orientational order parameter S and the angle ε in the mesophases of compound **12**.

$$\Delta\nu^F_{\xi\xi} = \Delta\nu^F_C S$$

where $\Delta\nu^F_C = -15.08$ ppm is an interaction constant defined by the geometry of the ring C. We assume that the ring C is deformed by the fluorine substituent which is indicated elsewhere in the literature.[21] In order to get an agreement between the results obtained from different techniques (^{13}C- and ^{1}H-NMR) the following interatomic distances have been used $r_{CF} = 1.344$ Å, $r_{CH} = 1.09$ Å. The interaction of the fluorine with hydrogen in position 12 is weak and appears as a small splitting of the triplet lines.

The angle ε (Scheme 2) between the molecular long axis and a *para*-axis of ring A was calculated from the splitting of the fluorine in position 2. In this case the splitting depends on the order parameter S as well as on the orientation of the *para*-axis of the ring A:

$$\Delta\nu^F_{\xi\xi} = \Delta\nu^F_A S\left(\frac{3}{2}\cos^2(\varepsilon) - \frac{1}{2}\right)$$

where the splitting constant $\Delta\nu^F_A = -28.0$ ppm. The shape of the ^{19}F-NMR spectra changes considerably upon the $B_2 \rightarrow B_{5F}$ and $B_{5A} \rightarrow B_{5F}$ phase transitions (Fig. 2). Sharp peaks could be observed only in the high temperature phase. After the transition into the B_{5A} phase the splitting of the fluorine in position 2 broadens which complicates the determination of the angle ε. The observed tendency of the splitting enables us to assume that the angle ε in the low temperature phases has similar values to those in the high temperature phase (Fig. 3). The angle ε was found to be 31–32°; this corresponds to a bending angle α (the angle between the wings of the molecule) of 116–118°. As shown in Fig. 3 the order parameter S is nearly temperature independent in the B_2 phase. At the transition into the B_{5A} phase S slightly increases. In the B_{5F} phase S reached a value of about 0.9.

X-Ray investigations

Although the compounds under investigation possess quite a large number of mesophases, only two kinds of X-ray patterns could be observed: one typical of the SmC or B_2 and the other one typical of the B_5 phases. The appearance of the X-ray patterns of both compounds is similar and they will be described for compound **12**. In the first, high-temperature

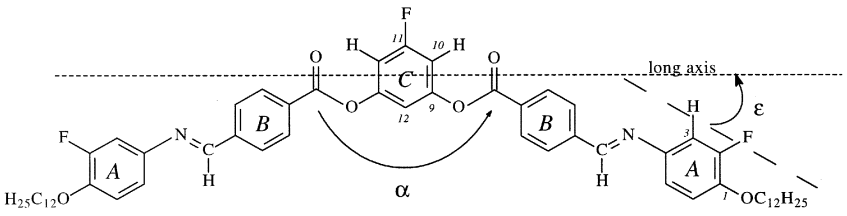

Scheme 2

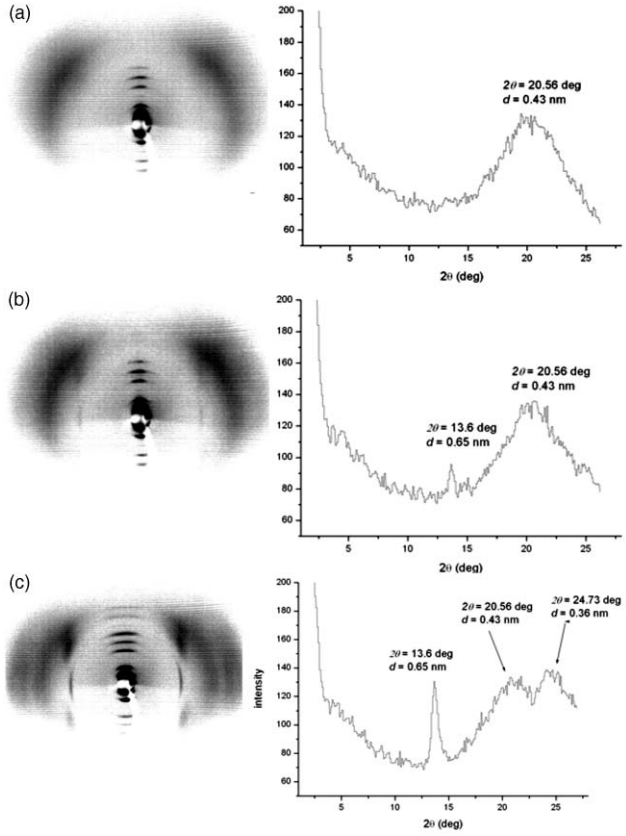

Fig. 4 X-Ray patterns of oriented samples and the equatorial scans (a) B_2 phase (135 °C), (b) B_{5A} phase (124 °C) and (c) B_{5F} phase (115 °C).

phase, up to six orders of layer-reflections have been seen from the diagrams of the surface-oriented samples where the third order reflection is of extreme low intensity (not detectable). In the wide-angle region there is a diffuse scattering with a maximum off the equator indicating liquid-like order within the smectic layers and the tilt of the molecules is characteristic for the SmC or B_2 phase (Fig. 4a). A polar order of the phase has been proved by electro-optical measurements, which indicates that the phase is, actually, B_2. The tilt angle ψ estimated from the positions of the diffuse maxima is $38 \pm 3°$ for the compound **12**. The equatorial scan for this compound shows only one broad maximum at a scattering angle of $2\theta \cong 20.6°$ in the diagram of the B_2 phase. Upon the transition from the B_2 phase into the lower-temperature phase, a narrow line

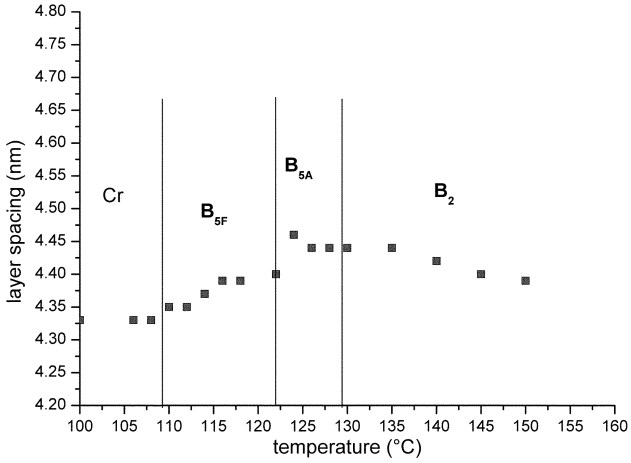

Fig. 6 Temperature dependence of the layer spacing of compound **12**.

perpendicular to the equator appears (Fig. 4b and 5). However, the diffuse scattering remains showing a considerably high amount of disorder in the phase. During cooling, an additional maximum is visible at a scattering angle around $2\theta \cong 24.7°$ (Fig. 4c). Those lines indicate an additional order within the smectic layers, which can be described by a rectangular lattice on a short-range scale with the parameters $a \cong 0.65$ nm and $b \cong 0.35$ nm. Thus, we observed that there are two kinds of scattering centers in the low-temperature phases: ordered in a rectangular two-dimensional lattice (the molecules from different layers are not correlated) and disordered centers which give a broad diffuse halo. Such behavior is characteristic for B_5 phases. No discontinuous change has been seen at the phase transition temperatures observed in the DSC below B_2 phase. The same situation has been observed for both compounds **12** and **8**. The layer spacing d, obtained from the powder samples, is nearly independent of the temperature for the compound **8**, whereas in the compound **12** a slight temperature dependence of the d-values has been found (Fig. 6).

After crystallization the diffuse scattering is absent, and only the reflections along the two lines remain. However, in the crystalline phase the intensity of the lines is modulated due to the positional correlation between the molecules from different layers.

Electro-optical investigations

Above the threshold the initial bright birefringent ribbon texture of the B_2 phase transforms into a smooth SmA-like

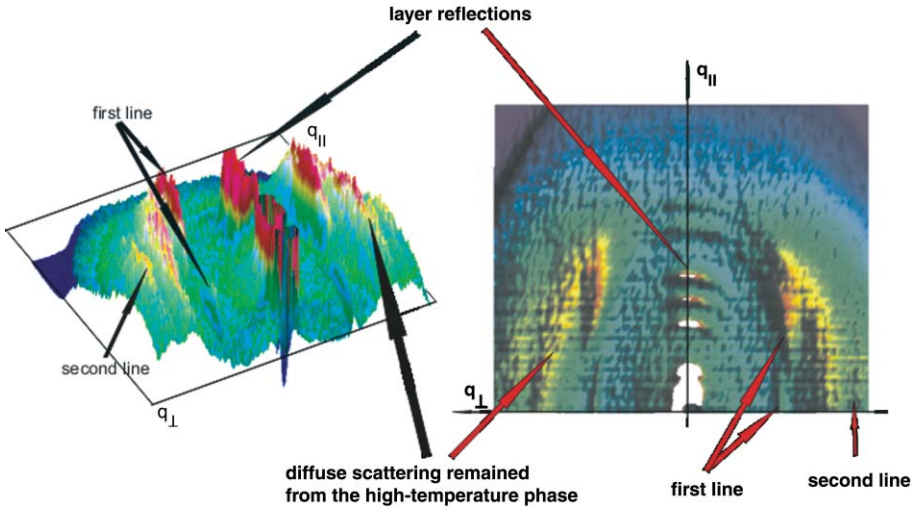

Fig. 5 Three-dimensional plot of an X-ray pattern in the B_{5F} phase (115 °C): a) perspective view, b) view from top (only upper half of the scattering sphere).

fan-shaped texture. When the field is removed, the texture switches back into the initial state. The textures of the switched state are independent of the sign of the applied field, which points to a racemic ground state. At the transition from the B_2 into the B_{5A} phase the threshold slightly increases from 0.6 V μm^{-1} till 1.3 V μm^{-1}, however the change of the textures on switching looks similar to the case of the B_2 phase (Fig. 7).

The electric response in the B_2 phase is quite unusual for both compounds **12** and **8**: it consists of a peak at low field and a double peak in a high-field region (Fig. 8a). The second high-field peak is broader than the first one, it broadens at lower temperature and completely disappears upon the transition into the B_{5A} phase (Fig. 8b).

A drastic change of the electro-optical behavior is observed in the low-temperature phase designated as B_{5F}. As seen from Fig. 8c, at the transition from B_{5A} into B_{5F} a third current peak comes out between the two peaks of the antiferroelectric B_{5A} phase; the latter diminish and disappear. Simultaneously, the single peak of the B_{5F} phase shifts towards higher values of τ which corresponds to an increasing threshold field (Fig. 8d). Furthermore, the texture of the switched states does not relax or change anyway when the external field is removed. The switching into another polarized state takes place only when the field of opposite polarity (higher than the threshold field) is applied. In contrast to the B_2 and B_{5A} phases, the textures of the switched states are different for opposite signs of the electric field, that means, dark domains became bright and *vice versa*. (Fig. 9) The brushes in the extinction cross in circular domains turn to an angle of about 65°, which corresponds to double the director tilt angle. There is a remarkable difference between the appearance of the antiferroelectric B_{5A} phase on cooling and heating. On heating from the B_{5F} phase, some homochiral domains remain, where the texture is different for an opposite sign of the applied field. In contrast, on cooling from B_2 the B_{5A} phase appears as a racemic one. In the B_2 phase only a racemic ground state has been observed.

Considering all experimental findings we can assume that the low temperature phase B_{5F} is ferroelectric. The hysteresis curves acquired by integration of the current response curves are shown in Fig. 10. The spontaneous polarization does not change considerably between the B_2, B_{5A} and B_{5F} phases (Fig. 11). On average there is no difference in the values of $\boldsymbol{P}_s$ between the compounds **12** and **8**. The low-temperature phase of the compound **8** also has a one-peak current response curve, although the polarized state slowly relaxes after the field is removed.

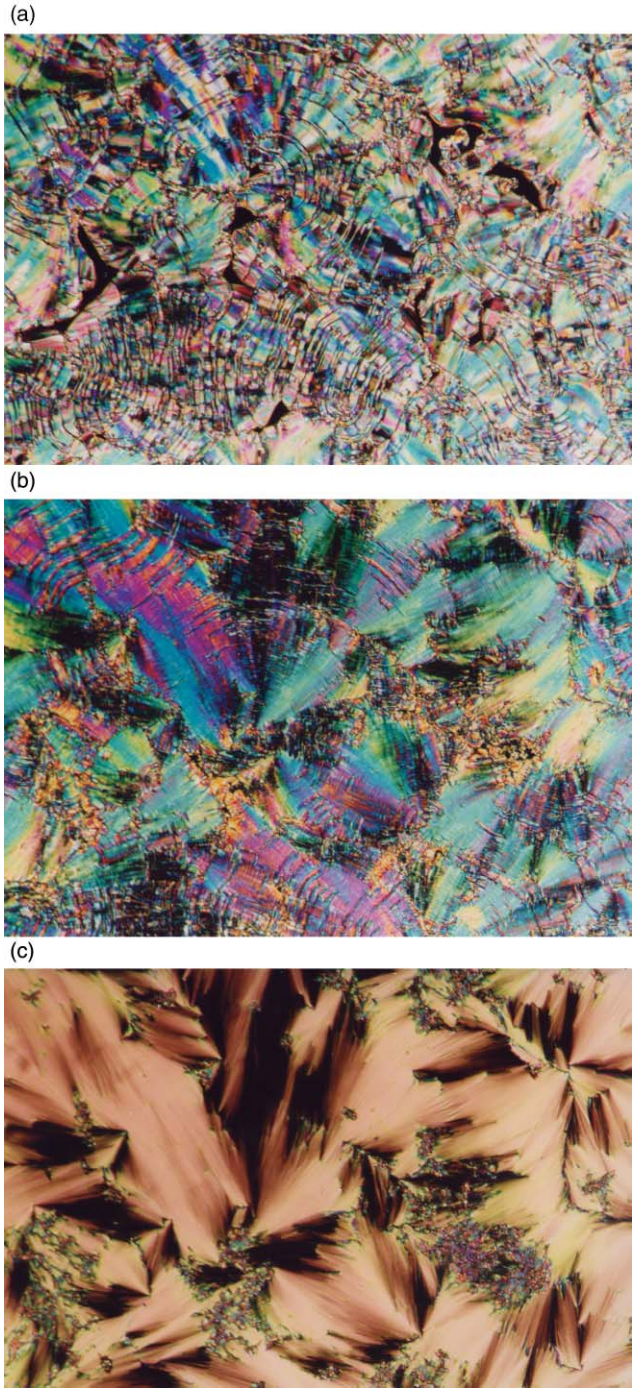

Fig. 7 Optical textures of the B_{5A} phase of compound **12** at 125 °C: a) $E = 0$ V μm^{-1}, b) $E = 0.6$ V μm^{-1}, c) $E = 1.6$ V μm^{-1}.

Discussion

To analyze the experimental results four arrangements have been modeled. A model of a molecule of compound **12** in an energy-minimum conformation was put into an orthorhombic body centered lattice. For the four structures: AFE synclinic $\{(x,y,z,)(-x,y,1/2z)\}$, AFE anticlinic $\{(x,y,z)(-x,-y,1/2z)\}$, FE synclinic $\{(x,y,z,)(x,y,1/2z)\}$, FE anticlinic $\{(x,y,z,)$-$(x,-y,1/2z)\}$ the X-ray patterns have been simulated (the terms synclinic and anticlinic correspond to the molecular tilt in neighboring layers and are expressed by the sign of the *y*-coordinate, whereas AFE/FE order is expressed by the sign of the *x*-coordinate). An example of AFE synclinic structure is shown in Fig. 12 and 13. Although the calculations were done on the crystalline structures, they still show the main features of the experimentally observed X-ray patterns. Introduction of the thermal fluctuations as well as the decrease of the interlayer correlations will smear out the reflections in the wide-angle region, as was observed experimentally.

Obviously, the difference between theses structures influences the intensity of (*hkl*) reflections with $l = 2n + 1$ and does not affect (00*l*) reflections. Since (*hkl*) reflections are absent in structures without interlayer correlation which actually takes place in the case of smectic liquid crystals, it is not possible to differentiate such structural nuances as AFE–FE, synclinic–anticlinic or helical ordering of the smectic layers on the basis of ''conventional'' X-ray studies. Therefore, there can be many B_5-like sub-phases which differ in the direction of the molecular tilt.

Inclining the molecule with respect to the layer normal, the calculated intensity of the meridian (00*l*) reflections changes, and at the tilt angle $\psi \approx 38$–$42°$ the intensity of the (003) reflection becomes very low in agreement with our experimental data (Fig. 14). Assuming that such model describes a crystalline state, an additional modification by the high Debye–Waller factor will increase the effect of extinction.

Another way to estimate the tilt angle comes from the ratio of the layer spacing *d* to the length of the molecule. Taking *L*

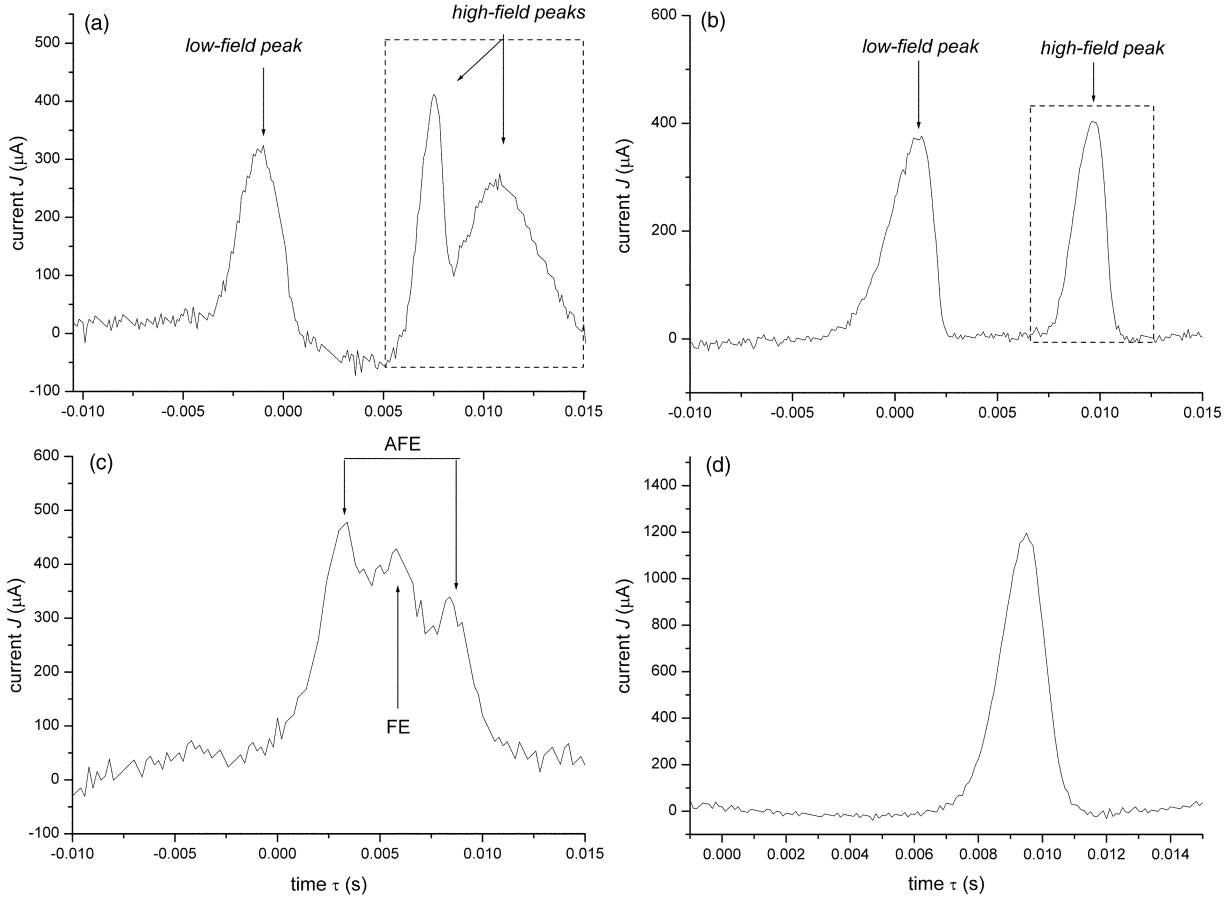

Fig. 8 Repolarization current of (a) the B_2 phase (136 °C), (b) the B_{5A} phase (124 °C), (c) at the transition $B_{5A} \rightarrow B_{5F}$ (122 °C), (d) the B_{5F} phase (117 °C) of compound **12**.

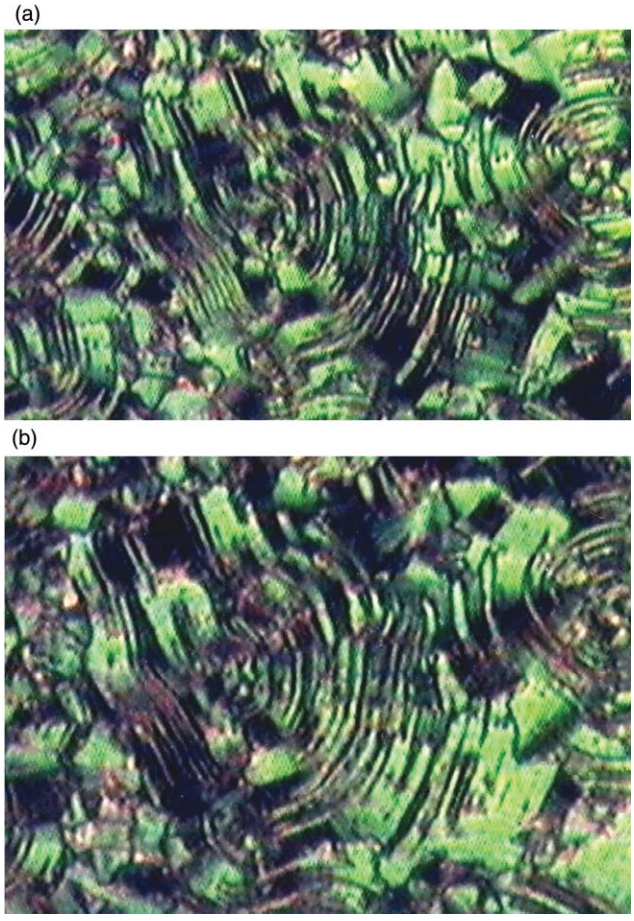

Fig. 9 Optical textures of the B_{5F} phase at 112 °C: (a) $E = +7.0$ V μm^{-1}, (b) $E = -7.0$ V μm^{-1}.

as the length of the stretched molecule, then the effective length is determined by $L_{\text{eff}} = L\sqrt{[2(1 - \cos\alpha)]}$, which describes the length of a bent molecule with the angle α at the apex. From NMR experiments the angle α has been estimated to be ~114 deg. With $L = 6.3$ nm, $L_{\text{eff}} = 5.3$ nm and the layer thickness $d = 4.3$ nm the result is $\psi = 36°$, which is in good agreement with the tilt angle obtained from outer-diffuse scattering and molecular modeling.

Electro-optical measurements employed triangular-wave

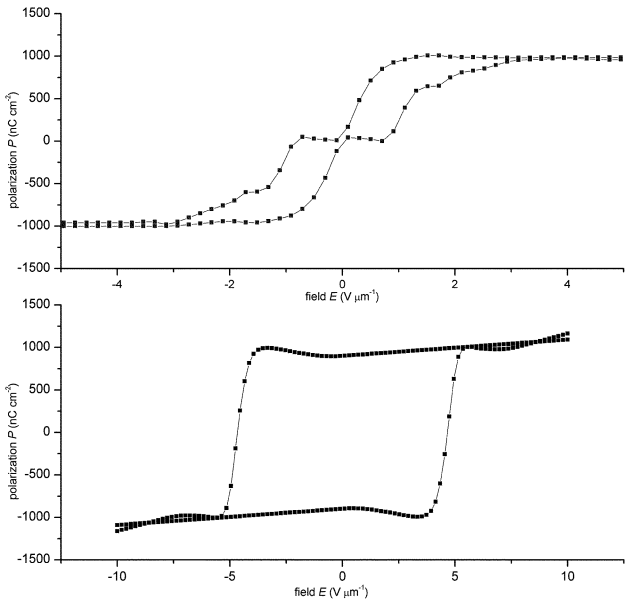

Fig. 10 Hysteresis curves $P(E)$ in (top) the antiferroelectric B_{5A} phase and (bottom) ferroelectric B_{5F} phase.

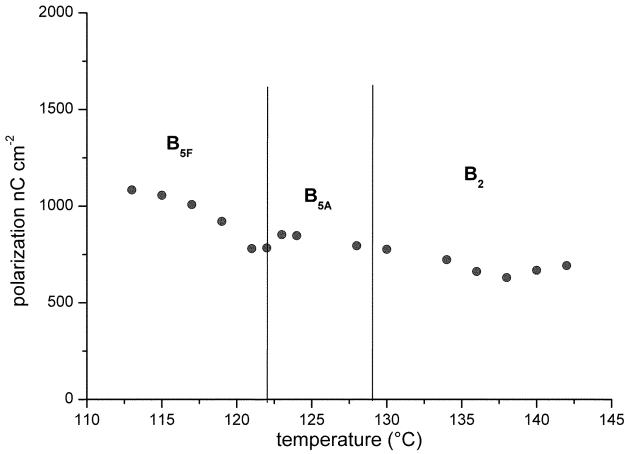

Fig. 11 Temperature dependence of the spontaneous polarization of compound **12**.

technique has shown that the high temperature B_{5A} phase of **12** is antiferroelectric and has a synclinic ground state. On the other hand the low-temperature B_{5F} phase is ferroelectric and synclinic. As has been mentioned above, the difference between the two phases cannot be detected in "conventional" X-ray experiments. The case of the compound **8** is similar, although the ferroelectric property of the low-temperature B_5 phase has not been conclusively proved. The occurrence of the AFE and FE phases in calamitic chiral compounds is quite well investigated[2,3,22] and there is a number of theoretical works on ferro-, antiferro- and ferri-electricity in liquid crystals. However, reviewing the experimental data on calamitic and bent-core compounds one can notice that ferroelectric phases are more usual for calamitics,[22] and antiferroelectric phases are common for "banana phases".[16] A naïve illustration of such phenomena can be given, similarly to a discussion in Lagerwall's book.[22] Let us consider fluctuations in the smectic layers involving partial permeation of molecules from layer to layer. In calamitic compounds such fluctuations are permitted by the synclinic order (Fig. 15a) and they themselves stabilize this order. Out-of-layer fluctuations give a thermodynamic

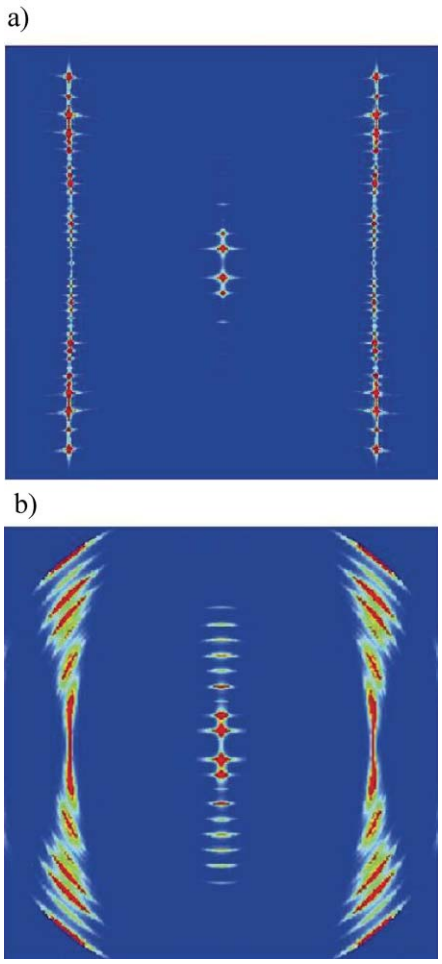

Fig. 13 Simulated pattern of the AFE synclinic structure a) without mosaicity, b) with mosaicity 5°.

(entropic) driving force for synclinic order, which is ferroelectric. In contrast, anticlinic stacking suppresses the out-of-layer fluctuations and thus carries an entropic penalty. Thus,

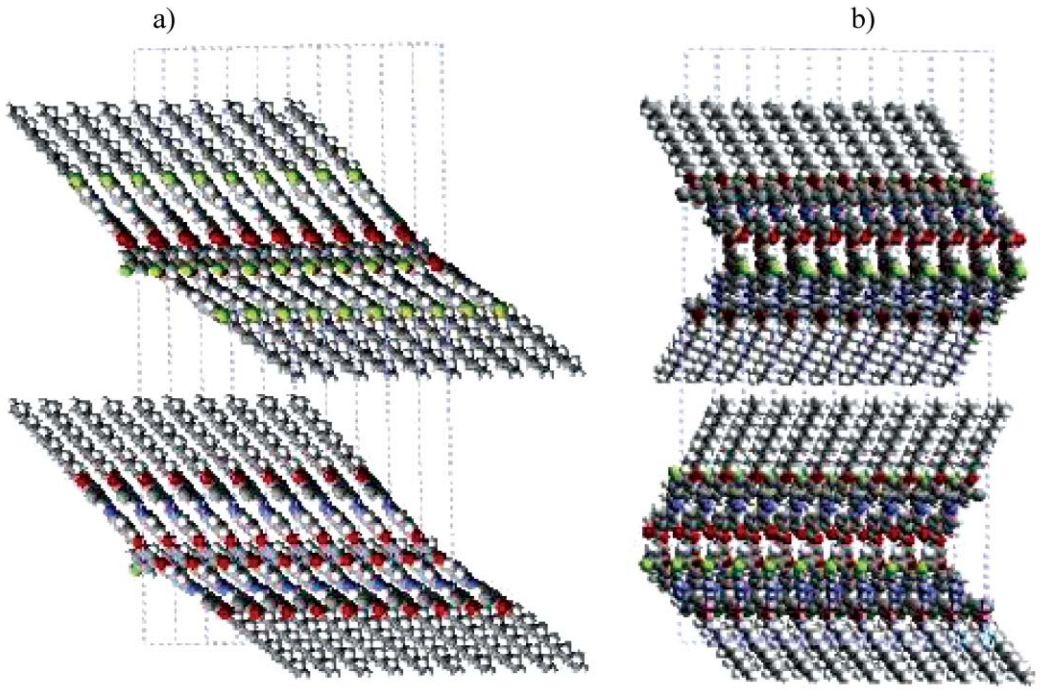

Fig. 12 Structural models a) front view of an AFE synclinic packing, b) side view of an AFE synclinic packing.

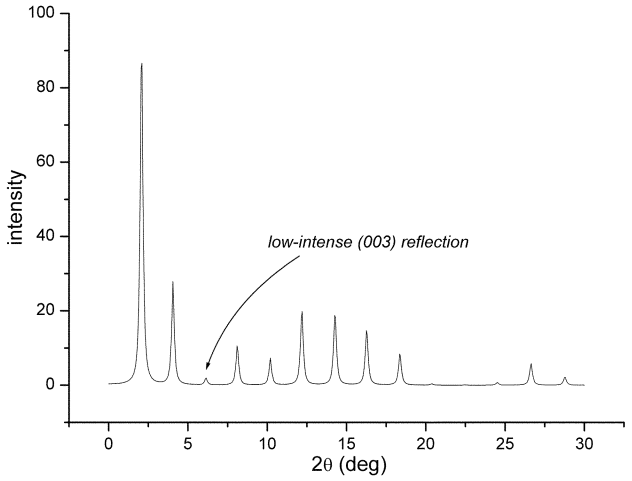

Fig. 14 Simulated intensity of (00*l*) reflections of an AFE synclinic model with the molecules tilted by an angle 40°.

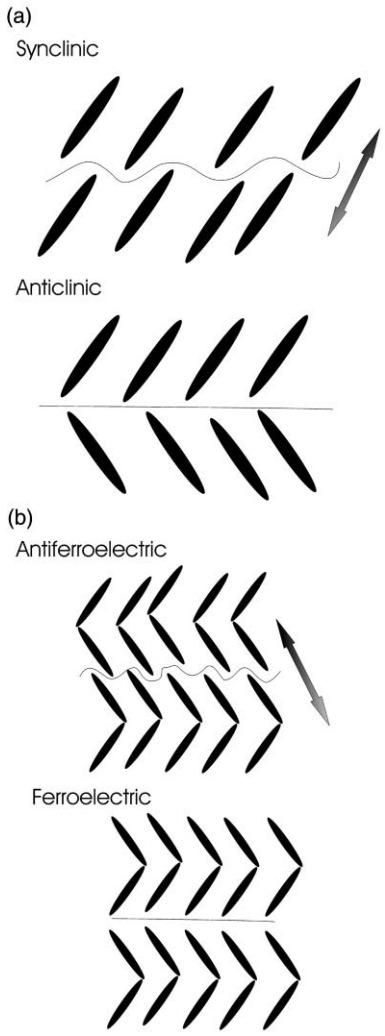

Fig. 15 Fluctuations in (a) synclinic and anticlinic structures of calamitics and (b) AFE and FE structures with bent-core mesogens.

the ferroelectric phase is the high-temperature one and the antiferroelectric phase occurs at lower temperatures in compounds with rod-like molecules. In the case of bent molecules the same argument is valid if we consider each smectic layer as a connected pair of anticlinically arranged rods (Fig. 15b). Then the penetration of the layers is favorable in an AFE arrangement of the molecules—but not in FE, which means that AFE phases are preferable. Regarding the tilt of molecules synclinic order has higher entropy. This is consistent with our observations that the most frequently observed B_2 (SmCP) and B_5 phases are antiferroelectric and synclinic (racemic), rarely anticlinic antiferroelectric; the ferroelectric B_{5F} phase observed in compound **12** is still synclinic and occurs at the temperature lower than AFE B_{5A} phase.

A closer look at the DSC curve made on heating of compound **12** (as well as **8**) reveals some sub-phases between B_{5A} and B_{5F}. A small temperature range of these sub-phases complicates a thorough investigation. Yet the following features have been found: (1) the sub-phases occur between antiferroelectric and ferroelectric phases; (2) they exist in quite narrow temperature intervals; (3) they are hardly noticeable by polarized microscope; (4) they can be seen on the DSC curve, however indistinguishable in X-ray.

This behavior is reminiscent of the behavior of ferrielectric phases SmC^*_γ, *etc.*, which differ in the sequence of the anticlinic and synclinic layers, and appear as a result of a competition between two different interactions: one favoring ferroelectric order and the other favoring antiferroelectric order. Although there might be some other explanations, to explore these sub-phases and ascertain their structure further investigations such as resonant X-ray techniques are required.

Experimental

The thermal behavior was investigated using a Perkin-Elmer Pyris 1 differential scanning calorimeter. The textures and the field-induced texture changes were examined using a polarizing microscope (Leitz Laborlux) equipped with a Linkam hot-stage (THM 600/S).

The electro-optical measurements were carried out using commercial ITO cells (EHC). The spontaneous polarization was measured using the triangular wave voltage method.

X-Ray diffraction measurements on non-oriented samples were done with a Guinier camera as well as a Guinier goniometer (Huber Diffraktionstechnik GmbH). Oriented samples were obtained by very slow cooling of a drop of the mesogen from the isotropic into the liquid-crystalline state on a glass plate. In this case the smectic layers could be aligned parallel to the substrates and the X-ray beam was incident parallel to the smectic layers. The X-ray patterns were recorded using a 2 D area detector (HI Star, Siemens AG).

NMR experiments were made using Bruker MSL500 spectrometer operating at 500 MHz for proton resonance. The temperature of the sample was stabilized with an accuracy of 0.1 °C. ^{13}C-NMR spectra at 125.6 MHz were recorded in the isotropic state using pulse excitation together with continuous or WALTZ decoupling method. For the liquid crystalline state, a cross polarization technique with higher decoupling power was used, however not all lines could be resolved. The order parameters and some conformational features were estimated mostly on the basis of ^{19}F-NMR experiments.

The structure model has been proposed on the basis of X-ray pattern simulation using CERIUS2 software and comparing it with the experimental data as described in ref. 23.

Acknowledgement

We gratefully acknowledge B. I. Ostrovskij for useful and stimulating discussions. This work was supported by the Deutsche Forschungsgemeinschaft (DFG) and Fonds der Chemischen Industrie.

References

1 R. B. Meyer, L. Liebert, L. Strzelecki and P. Keller, *J. Phys. (Fr.) Lett.*, 1975, **36**, L69.
2 A. P. L. Chandani, Y. Ouchi, H. Takezoe, A. Fukuda,

H. Tereshima, K. Furukawa and A. Kishi, *Jpn. J. Appl. Phys.*, 1989, **28**, L1261.
3 A. Fukuda, Y. Takanishi, T. Isozaki, K. Ishikawa and H. Takezoe, *J. Mater. Chem.*, 1994, **4**, 997.
4 J. Prost and P. Barois, *J. Chim. Phys.*, 1983, **80**, 65.
5 R. G. Petschek and K. M. Wiefling, *Phys. Rev. Lett.*, 1987, **59**, 343.
6 F. Tournilhac, L. Bosio, J.-F. Nicoud and J. Simon, *Chem. Phys. Lett.*, 1988, **145**, 452.
7 H. R. Brand, P. Cladis and H. Pleiner, *Macromolecules*, 1992, **25**, 7223.
8 L. Lin, *Mol. Cryst. Liq. Cryst.*, 1987, **146**, 41.
9 F. Tournilhac, L. M. Blinov, J. Simon and S. V. Yablonski, *Nature*, 1992, **359**, 621.
10 E. A. Soto Bustamente, S. V. Yablonski, B. I. Ostrovski, L. A. Beresnev, L. M. Blinov and W. Haase, *Liq. Cryst.*, 1996, **21**, 829.
11 T. Niori, F. Sekine, J. Watanabe, T. Furukawa and H. Takezoe, *J. Mater. Chem.*, 1996, **6**, 1231.
12 W. Weissflog, Ch. Lischka, I. Benne, T. Scharf, G. Pelzl, S. Diele and H. Kruth, *Proc. SPIE – Int. Soc. Opt. Eng.*, 1998, **3319**, 14.
13 S. Diele, S. Grande, H. Kruth, Ch. Lischka, G. Pelzl, W. Weissflog and I. Wirth, *Ferroelectrics*, 1998, **212**, 169.
14 A. Jakli, S. Rauch, D. Lötzsch and G. Heppke, *Phys. Rev. E.*, 1998, **57**, 6737.
15 D. R. Link, G. Natale, R. Shao, J. E. Maclennan, N. A. Clark, E. Körblova and D. M. Walba, *Science*, 1997, **278**, 1924.
16 G. Pelzl, S. Diele and W. Weissflog, *Adv. Mater.*, 1999, **11**, 707.
17 D. M. Walba, E. Körblova, R. Shao, J. E. Maclennan, D. R. Link, M. A. Glaser and N. A. Clark, *Science*, 2000, **288**, 2181.
18 H. T. Nguyen, J. C. Rouillon, J. P. Marcerou, J. P. Bedel, P. Barois and S. Sarmento, *Mol. Cryst. Liq. Cryst.*, 1999, **328**, 177.
19 W. Weissflog, H. Nádasi, U. Dunemann, G. Pelzl, S. Diele, A. Eremin and H. Kresse, *J. Mater. Chem.*, 2001, **11**, 2748.
20 A. Eremin, I. Wirth, S. Diele, G. Pelzl, H. Schmalfuss, H. Kresse, H. Nádasi, K. Fodor-Csorba, E. Gács-Baitz and W. Weissflog, *Liq. Cryst.*, 2002, in the press.
21 S. Doraiswamy and S. D. Sharma, *J. Mol. Struct.*, 1983, **102**, 81.
22 S. T. Lagerwall, *Ferroelectric and Antiferroelectric Liquid Crystals*, Wiley-VCH, Weinheim, New York, Chichester, Brisbane, Singapore, Toronto, 1999.
23 A. Eremin, S. Diele, G. Pelzl, H. Nádasi, W. Weissflog, J. Salfetnikova and H. Kresse, *Phys. Rev. E*, 2001, **64**, 51707.